

Ultrasoft spin-dependent pseudopotentials

Vincent Cocula

Department of Chemistry and Biochemistry, University of California, Los Angeles, California 90095-1569

Chris J. Pickard

Theory of Condensed Matter (TCM) Group, Cavendish Laboratory, Madingley Road, Cambridge, CB3 0HE, United Kingdom

Emily A. Carter^{a)}

Department of Mechanical and Aerospace Engineering and Program in Applied and Computational Mathematics, Princeton University, Princeton, New Jersey 08544-5263

(Received 16 August 2005; accepted 21 September 2005; published online 2 December 2005)

The use of the spin-dependent pseudopotentials has been shown to markedly enhance the transferability of the commonly used spin-neutral pseudopotential method for the study of the structural and magnetic properties of transition-metal-containing materials. Unfortunately, because the method was based on the rather expensive norm-conserving pseudopotential formalism, the method was limited to the study of fairly small systems. Here we present an extension of the spin-dependent pseudopotential method for the far more computationally advantageous ultrasoft formalism and show that it is very easy to add such a feature to any preexisting computer code. We benchmark our new method by comparing to previously published results and then apply it to the study of several relevant test cases: bulk Ni, Fe, and Co, as well as a Pd atomic wire.

© 2005 American Institute of Physics. [DOI: [10.1063/1.2121547](https://doi.org/10.1063/1.2121547)]

I. INTRODUCTION

With the ever increasing computational power available, quantum-mechanical modeling of condensed matter has become a powerful tool for studying the physical properties of various types of materials. Such methods now can be routinely performed on quite large systems (hundreds of atoms), thereby allowing the study of phenomena at the nanoscale. Moreover, when combined with methods to bridge length scales (such as finite-element methods), quantum-mechanical simulations also are starting to provide a valuable tool to accurately describe regions of a macroscopic piece of material where information at the atomic level is important.¹⁻³

The most accurate first-principles methods used in condensed matter are usually based on the density-functional theory^{4,5} (DFT) and often employ a plane-wave basis set, three-dimensional periodic boundary conditions, and fast Fourier transforms (FFTs) to represent quantities in both real and reciprocal spaces.⁶ Those methods can be divided into two major categories: the all-electron (AE) and pseudopotential⁷ (PsP) types. AE methods explicitly account for all electrons in the system, usually employing a mixed basis set in which the plane waves are augmented around each ionic species in order to describe the complex features of the wave function near the nuclei. Although AE methods are very accurate, they are also generally quite expensive. By contrast, PsP methods are approximations to the AE case that dramatically reduce the cost associated with such simulation and are based on the fact that the electronic states of an atom generally are well separated energetically into discrete core

and valence electronic states. Since only valence electrons significantly contribute to the bonding and many other properties, it is therefore tempting to reduce the AE problem to one of pseudoatoms in which only valence electrons are taken into account explicitly in the DFT equations.

Such pseudopotentials are derived from first-principles calculations on isolated atoms, where one first performs an AE calculation in order to get the AE wave functions and eigenenergies. Then a new set of so-called pseudo-wave-functions is constructed so that within some core cutoff radius r_c , often corresponding to the outermost extremum of the AE wave function, the AE wave functions are smoothed out to obtain smooth and nodeless pseudo-wave-functions. Beyond this cutoff radius, and because it is desirable that the atomic properties are correctly described in the valence region, the pseudo-wave-functions are set to match the AE ones. With this new set of functions, one then inverts the DFT equations on the pseudoatom to solve for the effective, screened pseudopotential, a smooth, nonsingular, and non-Coulombic function near the nucleus. Because the pseudo-wave-functions are smooth functions near the nucleus, it is possible to expand them very easily using a plane-wave basis set, thus dramatically simplifying the formalism normally involved in AE methods. An exception is the projector augmented wave (PAW) method,⁸ which may be considered an AE method in the frozen-core approximation; the PAW method retains the efficiency of pseudopotential schemes.

These PsP methods can be subdivided further into two categories: the so-called norm-conserving⁹ and ultrasoft¹⁰ PsPs. In the former, the norm of the pseudo-wave-function is set equal to that of the AE wave function, ensuring conservation of the total valence charge of the pseudoatom. In the

^{a)} Author to whom correspondence should be addressed. Electronic mail: eac@princeton.edu

latter, the norm-conservation constraint on the pseudo-wave-function is relaxed and instead an optimally smooth wave function is generated. In this case, the deficit of valence charge is recovered self-consistently using the so-called augmentation functions.

Although PsP methods are an approximation to the AE case, they have been shown to yield results very similar to AE methods, and years of development of the method have made it a very efficient, accurate, and robust tool for studying the electronic properties of materials. Nevertheless, the otherwise reliable PsP theory frequently produces unsatisfactory results (in the sense of being highly sensitive to parameter choice) for the case of transition elements,^{11,12} and as a consequence, the method has been used sparingly for transition-metal-containing materials. For such materials, AE theories are often preferred because they have been found to be more reliable.

The unique properties of transition elements present many pitfalls for the pseudopotential approximation. First, they are open-shell systems. Pseudopotentials are usually spin averaged so that they do not explicitly account for the variety of electronic spin states that may be adopted by the element. As a consequence, such spin-averaged pseudopotentials generally do a poor job at describing the magnetic properties of transition-metal-based materials. Secondly, they exhibit nearly degenerate ns and $(n-1)d$ electronic shells, making it difficult to separate the atom into core and valence states. A non-negligible overlap between core and valence densities exists; for accurate calculations, it is sometimes necessary to treat the semicore p electrons as valence states, which comes with a considerable (possibly prohibitive) computational cost. Transition elements also exhibit very localized and sharp d wave functions, which makes it difficult to build much smoother pseudo-wave-functions than the original AE wave functions, producing very costly computations. Often, instead of using the outer maximum of the AE wave function, the cutoff radius for those d wave functions is set to be much larger in order to produce a smooth pseudo-wave-function. Unfortunately, because such a pseudo-wave-function does not resemble the AE one as well anymore, the transferability of the associated pseudopotential can be severely compromised. In fact, it was recently noted that only in the limit of short cutoff values, i.e., for expensive potentials, can one expect high accuracy for specific cases.¹³ This leaves one with the unfortunate choice of choosing a compromise cutoff value that allows for the best transferability possible at the least computational expense. Lastly, it has been shown that the implicit linearization of the exchange-correlation potential during pseudopotential generation dramatically affects their transferability for the specific case of transition elements.¹⁴ The problem can be partially fixed by using a non-uniquely-determined function, the so-called non-linear core correction (NLCC), introducing yet another parameter to be adjusted during the generation process. Although there seems to be no clear definition or choice for this parameter (the so-called NLCC cutoff, r_c^{NLCC}), it has an understandable influence on the accuracy (or lack thereof) of the resulting pseudopotential.^{12,15}

Thus, current implementations of pseudopotential theory

have a number of adjustable parameters, which can have significant impact on the behavior of the potential in both the atomic and solid states. While, in general, creating potentials with smaller core radii (and therefore slower convergence with basis set size) produces more accurate results, there appears to have been the temptation at times to use these apparent degrees of freedom to “fit” to experimental results. This is clearly an unsatisfactory situation for a supposedly first-principles method.

Given the above discussion, use of the term “first principles” to describe PsP theories will only be appropriate when further development¹¹ of the pseudopotential approximation allows us to get beyond the unreliable and far too common fiddling with the many parameters involved in the generation procedure. A few years ago, Watson and Carter proposed the use of a self-adaptive, multireference potential as a systematic way to improve on the pseudopotential transferability properties for transition elements with a minimum number of adjustable parameters.¹⁶ The present work deals with the applicability and accuracy of those so-called spin-dependent pseudopotentials for transition-metal-containing materials when combined with the computationally advantageous Vanderbilt ultrasoft pseudopotentials.¹⁰ We show here that greater accuracy can be achieved for spin-polarized systems within this theory, without the need to use computationally demanding basis sets or submitting to the temptation to adjust parameters.

The paper is organized as follows. Section II gives the theoretical background of the spin-dependent pseudopotential method. We then show in Sec. III how the method can be incorporated conveniently within the ultrasoft scheme. Section IV gives the general computational details, and we finally present in Sec. V the results given by the method when compared to previous theories. Section VI provides concluding remarks.

II. METHOD

The spin-dependent pseudopotentials (SDPs) were proposed originally by Watson and Carter. They are based on a multireference pseudopotential approach that aims to capture core relaxation effects and valence shell spin and spatial variations via a self-consistent perturbation to the commonly used spin-neutral pseudopotentials. Although transition elements are open-shell atomic species, pseudopotentials have been generated traditionally using their spin-neutral (i.e., nonmagnetic) ground-state electronic configuration, giving rise to a single potential v^ρ affecting both up- and down-spin components of the Kohn-Sham Hamiltonian. Then the total ionic energy becomes

$$E^{\text{ion}} = \int v^\rho(\mathbf{r})n(\mathbf{r})d\mathbf{r}, \quad (1)$$

where $n(\mathbf{r})$ is the total valence charge density. For open-shell systems, in reality the potentials affecting each spin channel should not be equal so that Eq. (1) should be generalized to

$$E^{\text{ion}} = \int [v^\uparrow(\mathbf{r})n^\uparrow(\mathbf{r}) + v^\downarrow(\mathbf{r})n^\downarrow(\mathbf{r})]d\mathbf{r}. \quad (2)$$

A spin-dependent pseudopotential must then have an explicit dependence through the spin density to reflect its direct dependence on the electronic population of both the up- and down-spin components of the wave function. We define our spin-dependent pseudopotential by

$$\begin{aligned} v^\uparrow(\mathbf{r}) &= v^\rho(\mathbf{r}) + F[\beta(\mathbf{r})]\delta v(\mathbf{r}), \\ v^\downarrow(\mathbf{r}) &= v^\rho(\mathbf{r}) + F[-\beta(\mathbf{r})]\delta v(\mathbf{r}), \end{aligned} \quad (3)$$

with a functional dependence $F[\beta(\mathbf{r})]$ on the local spin polarization $\beta(\mathbf{r})$ defined as

$$\beta(\mathbf{r}) = \frac{n^\uparrow(\mathbf{r}) - n^\downarrow(\mathbf{r})}{n^\uparrow(\mathbf{r}) + n^\downarrow(\mathbf{r})}. \quad (4)$$

In Eq. (3), v^ρ is the traditionally used spin-neutral reference potential and δv denotes the spin-dependent perturbation. By spin-neutral pseudopotential, we mean the potential derived for the atom in its nonmagnetic electronic configuration where both up- and down-spin channels are equally populated, i.e., for the s^2d^6 Fe atom, this would correspond to $s^{1\uparrow,1\downarrow}d^{3\uparrow,3\downarrow}$, where, e.g., the three up-spin d electrons are distributed equally among all five up-spin d orbitals to maintain spherical symmetry of the atom. By taking the functional $F[\beta(r)]$ to be simply equal to the local spin polarization $\beta(r)$, and then taking the functional derivatives of the energy, the expression for the spin-dependent pseudopotentials becomes

$$\begin{aligned} v^\uparrow(r) &= \frac{\delta E^{\text{ion}}}{\delta n^\uparrow(r)} = v^\rho(r) + \beta(r)(2 - \beta(r))\delta v(r), \\ v^\downarrow(r) &= \frac{\delta E^{\text{ion}}}{\delta n^\downarrow(r)} = v^\rho(r) - \beta(r)(2 + \beta(r))\delta v(r). \end{aligned} \quad (5)$$

The perturbation $\delta v(r)$ is chosen to be the spherically symmetric function

$$\delta v(r) = \frac{v^{\text{p}}(r) - v^\rho(r)}{\beta_{\text{at}}(r)(2 - \beta_{\text{at}}(r))}, \quad (6)$$

where the potential $v^{\text{p}}(r)$ is the pseudopotential affecting the majority spin of the fully polarized atom. For the case of the Fe atom, this would correspond to its $s^{1\uparrow,1\downarrow}d^{5\uparrow,1\downarrow}$ electronic configuration. In Eq. (6), β_{at} is the atomic local spin polarization derived from the fully polarized pseudoatom spin density. We now argue that this choice of $\delta v(r)$ is justified by considering the two limits of nonmagnetic and fully polarized atoms and the implications for transferability.

Because the spin-dependent pseudopotential is self-consistently adapted to the spin polarization locally adopted by the atom, it is expected to enhance the transferability of the overall potential. Moreover, the expression for the spin-dependent perturbation was specifically chosen so as to give the correct expression for the potential in the nonmagnetic and fully polarized limits. For example, if the calculation self-consistently converges towards a nonmagnetic configuration, then the corresponding self-consistent spin polarization $\beta(\mathbf{r})$ will vanish to zero. In this case, the spin-dependent potential affecting the atom simply reverts to

$$\begin{aligned} v^\uparrow(\mathbf{r}) &= v^\rho(\mathbf{r}), \\ v^\downarrow(\mathbf{r}) &= v^\rho(\mathbf{r}), \end{aligned} \quad (7)$$

which corresponds to the correct expression for the potentials in the nonmagnetic limit. In the other limit where the calculation converges to a fully polarized atomic configuration, the self-consistent spin polarization $\beta(\mathbf{r})$ equals or resembles the spherical $\beta_{\text{at}}(r)$ and the expressions for the potentials become

$$\begin{aligned} v^\uparrow(r) &= v^{\text{p}}(r), \\ v^\downarrow(r) &= v^\rho(r) - \frac{2 + \beta(r)}{2 - \beta_{\text{at}}(r)}(v^{\text{p}}(r) - v^\rho(r)). \end{aligned} \quad (8)$$

In this case, we see that the potential affecting the majority spin component of the atom is the potential affecting the majority spin of a fully polarized atom, which is the “exact” result. Note that the minority spin potential does not quite return the exact result; Watson and Carter noted this earlier and showed that the minority spins are not quite as well described as the majority spin electrons.¹⁶ For all other spin configurations, the self-consistent coefficient

$$\frac{\pm\beta(r)(2 \mp \beta(r))}{\beta_{\text{at}}(r)(2 - \beta_{\text{at}}(r))} \quad (9)$$

acts as a weight factor that produces a total pseudopotential containing more or less polarization.

The spin-dependent pseudopotentials were shown to describe very accurately the energetics of transition-metal atoms by enhancing the potentials’ transferability over the commonly used spin-neutral ones.¹⁶ The method was then extended to solid-state calculations in both real-space¹⁷ and reciprocal-space¹⁵ DFT codes. This formalism, based on norm-conserving pseudopotentials in the Kleinman-Bylander¹⁸ form was also shown to improve the pseudopotential method’s accuracy for transition-metal-containing materials. Unfortunately, the use of such norm-conserving pseudopotentials is quite expensive in the case of transition elements and does not allow widespread use of the method for large systems. This problem was solved by Vanderbilt via his introduction of the ultrasoft (spin-neutral) pseudopotentials¹⁰ that allow the study of significantly larger systems. Unfortunately, the ultrasoft pseudopotentials suffer from the same transferability problems as the conventional spin-neutral norm-conserving ones. The aim of this work is then to combine the improvements of the method due to the use of the spin dependence with the computationally advantageous ultrasoft pseudopotential scheme.

III. IMPLEMENTATION DETAILS AND GENERATION

The generation of Vanderbilt’s ultrasoft pseudopotentials¹⁹ (USPP) always start with an all-electron calculation of the isolated atom, where the one-dimensional radial DFT equations are solved,

$$(\hat{T} + \hat{V})\psi_{nl}(r) = \epsilon_{nl}\psi_{nl}(r). \quad (10)$$

Here the total potential \hat{V} includes the appropriate exchange-correlation potential [either the local-density approximation (LDA) or the generalized gradient approximation (GGA)] to be utilized during the solid-state calculation. For each $\{nl\}$ valence state explicitly included in the pseudopotential, a set of soft pseudo-wave-functions $\phi_{nl}(r)$ are then created such that they match the all-electron ones at and beyond some chosen cutoff radius r_{cl} . The Kohn-Sham equations are then inverted to solve for the total effective pseudopotential $V_{\text{eff}}^{\text{ps}}$ so that it satisfies the following set of equations:

$$(\hat{T} + V_{\text{eff}}^{\text{ps}})\phi_{nl}(r) = \epsilon_{nl}\phi_{nl}(r). \quad (11)$$

Note that at this point more than one reference energy ϵ_{nl} can be chosen per angular momentum, independent of whether the norm-conservation constraint is enforced for the pseudo-wave-function generation. We will therefore use a composite index i which stands for a set of $i = \{nl, \tau\}$, where $\tau = 1, 2, 3, \dots$ is the number of reference energies chosen per $\{nl\}$ valence state. The total effective pseudopotential is then separated into a local and nonlocal contribution,

$$V_{\text{eff}}^{\text{ps}}(r) = V_{\text{loc}}(r) + \sum_l \Delta v_l(r), \quad \Delta v_l = v_l - V_{\text{loc}}, \quad (12)$$

where V_{loc} contains the local pseudopotential for a chosen valence state, as well as the Coulombic, Hartree, and exchange-correlation contributions, and is set to match the AE Kohn-Sham potential at and beyond the core radius. By definition, the nonlocal parts of the potential are short-range angular corrections to the local part, vanishing at the cutoff radii r_{cl} . Once a smooth local potential has been chosen, a set of nonlocal projectors are created:

$$|\chi_i\rangle = (\epsilon_i - \hat{T} - V_{\text{loc}})|\phi_i\rangle, \quad (13)$$

from which we define a new set of basis functions β_i , dual to the pseudo-wave-functions ϕ_i ,

$$|\beta_i\rangle = \sum_j (B^{-1})_{ji}|\chi_j\rangle, \quad (14)$$

with the coefficients determined from

$$B_{ij} = \langle \phi_i | \chi_j \rangle. \quad (15)$$

The total nonlocal operator is then rewritten as

$$\hat{V}_{\text{NL}} = \sum_{i,j} B_{ij} |\beta_i\rangle \langle \beta_j|, \quad (16)$$

provided that the norm-conservation condition on the pseudo-wave-function

$$q_{ij} = \langle \psi_i | \psi_j \rangle - \langle \phi_i | \phi_j \rangle = 0 \quad (17)$$

is enforced.

We note that for the special case where only one reference energy is chosen per angular momentum, Eq. (16) simply reverts to the Kleinman-Bylander form of the separable nonlocal potential.¹⁸ Vanderbilt further showed that the norm-conservation of Eq. (17) can be dropped if one adopts a generalized eigenvalue problem of the form

$$(\hat{T} + \hat{V}_{\text{loc}} + \hat{V}_{\text{NL}})|\phi\rangle = \epsilon \hat{S} |\phi\rangle, \quad (18)$$

where the overlap operator \hat{S} is defined by

$$\hat{S} = 1 + \sum_{i,j} q_{ij} |\beta_i\rangle \langle \beta_j|, \quad (19)$$

where q_{ij} is the integral over all space of the augmentation function $Q_{ij}(r)$ representing the difference in norm between the all-electron wave-functions and pseudo-wave-functions,

$$Q_{ij}(r) = \psi_i(r)\psi_j(r) - \phi_i(r)\phi_j(r). \quad (20)$$

The new nonlocal operator \hat{V}_{NL} thus becomes

$$\hat{V}_{\text{NL}} = \sum_{i,j} D_{ij} |\beta_i\rangle \langle \beta_j|, \quad (21)$$

where the new coefficients are

$$D_{ij} = B_{ij} + \epsilon_j q_{ij}. \quad (22)$$

This formalism, far more complex than norm-conserving pseudopotentials in the Kleinman-Bylander form, makes it nontrivial to derive the exact expression that the ultrasoft spin-dependent potentials should take. As we saw in the previous section, the determination of our spin-dependent pseudopotentials requires the generation of two atomic potentials, one for the spin-neutral and the other for the fully polarized atomic configuration. Those will give rise to two distinct sets of all-electron wave-functions and pseudo-wave-functions, which makes it unclear how to accurately compute the augmentation functions from Eq. (20), or even the total nonlocal projector \hat{V}_{NL} of Eq. (21). Furthermore, such an implementation in a reciprocal-space DFT code would be anything but trivial. But since the major contribution of the pseudopotential arises from its local part, with the nonlocal operator only acting as short-ranged small corrections, we propose that applying the spin-dependent perturbation only to the local potential should be enough (the nonlocal part of the total pseudopotential is left to be equal to the spin-neutral nonlocal projectors). Three arguments support this claim. First, the nonlocal form of a potential is already an approximation to its semilocal form and is exact only for the very special case when the atom takes on the exact electronic configuration used for the pseudopotential generation, which is never true in the case of a solid-state environment. Therefore, neglecting the small spin-dependent perturbation on the already short-ranged nonlocal corrections should be reasonable. Second, aside from the nonlocal $D_{i,j}$ coefficients (which are expected to be small), only the local part of the potential is unscreened before its use in solid-state calculations,

$$v_{\text{loc}}(r) = V_{\text{loc}}(r) - v_H[n(r)] - v_{\text{xc}}[n(r)]. \quad (23)$$

Here v_H and v_{xc} are the Hartree and exchange-correlation potentials for the isolated atom. The inherent error due to the explicit linearization of the exchange-correlation potential only affects the local pseudopotential v_{loc} , and it is expected that the spin dependence will play a greater role in correcting those inherent errors. Finally, unlike the nonlocal channels, the local potential affects all electrons in the system and

TABLE I. Atomic parameters used for the ultrasoft pseudopotential generation. In all instances, the $l=1$ angular momentum channel was chosen for the local potential. See text for detailed explanations.

Element	PsP name	Nonmagnetic configuration	r_c (bohr)			r_c^{NLCC} (bohr) (if used)
			$r_{c,s}$	$r_{c,p}$	$r_{c,d}$	
Cr	SNP-I	s^1d^5	2.50	2.50	2.50	
Ni	SNP-I	s^2d^8	2.20	2.20	2.20	
Fe	SNP-I	s^2d^6	2.40	2.40	2.40	
	SNP-II	s^2d^6	2.40	2.40	2.40	1.68
	SNP-III ^a	$s^{1.75}p^{0.25}d^6$	2.20	2.00	2.00	1.40
Co	SNP-I	s^2d^7	2.20	2.20	2.20	
	SNP-II	s^2d^7	2.20	2.20	2.20	1.54
	SNP-III ^a	s^2d^7	2.41	2.41	2.41	
	SNP-IV ^a	$s^{1.95}p^{0.05}d^7$	2.10	2.10	2.00	1.70
Pd	SNP-I	s^1d^9	2.60	2.60	2.60	
	SNP-II	s^1d^9	2.60	2.60	2.60	1.82
	SNP-III ^a	s^0d^{10}	2.66	2.66	2.66	

^aDefault potentials provided with the CASTEP code.

using the spin-dependent perturbation only on the latter will still affect all electrons.

The implementation of our new method then becomes quite straightforward. First, a conventional spin-neutral ultrasoft pseudopotential is generated, leading to the quantities defining the potential: the total effective local pseudopotential V_{loc}^o , the beta projectors $|\beta_i^o\rangle$, the nonlocal coefficients D_{ij}^o and the augmentation functions $Q_{ij}^o(r)$.²⁰ We then generate another pseudopotential using the exact same parameters as for the spin-neutral one, but for the fully polarized electronic configuration of the atom, leading to $V_{\text{loc}}^{\text{fp},\uparrow\downarrow}$ —all other nonlocal quantities being discarded [that is, $|\beta_i^{\text{fp},\uparrow\downarrow}\rangle$, $D_{ij}^{\text{fp},\uparrow\downarrow}$, and $Q_{ij}^{\text{fp},\uparrow\downarrow}(r)$]. Only the majority spin component of the local potential is then kept, e.g., $V_{\text{loc}}^{\text{fp},\uparrow}$, where both local potentials are then unscreened in the traditional fashion,

$$\begin{aligned} v_{\text{loc}}^o(r) &= V_{\text{loc}}^o(r) - v_H[n^o] - v_{\text{xc}}[n^o], \\ v_{\text{loc}}^{\text{fp},\uparrow}(r) &= V_{\text{loc}}^{\text{fp},\uparrow}(r) - v_H[n^{\text{fp}}] - v_{\text{xc}}[n^{\text{fp}}], \end{aligned} \quad (24)$$

where n^o and n^{fp} are the respective charge densities of the spin-neutral and fully polarized pseudoatom. The coefficient $\beta_{\text{at}}(r)$ is then computed from $n^{\text{fp},\uparrow\downarrow}$ following Eq. (4) and the spin-dependent perturbation is constructed as in Eq. (6). Both $v_{\text{loc}}(r)$ and $\delta v_{\text{loc}}(r)$ are then Fourier transformed for input onto the reciprocal-space grid of the solid-state DFT code. In such codes, the ion-electron energy is often conveniently evaluated in real space, where the total local potential $v_{\text{loc}}(\mathbf{G})$ is Fourier transformed back into real space and multiplied by the self-consistent charge density. In order to evaluate the spin-dependent potential energy, we also transform back $\delta v_{\text{loc}}(\mathbf{G})$ so that, along with the self-consistent local spin polarization $\beta(\mathbf{r})$ obtained from the self-consistent charge densities $n^{\uparrow\downarrow}(\mathbf{r})$, we obtain

$$\begin{aligned} E^{\text{ion},\uparrow} &= \int [v_{\text{loc}}^o(\mathbf{r})n^{\uparrow}(\mathbf{r}) + \beta(\mathbf{r})(2 - \beta(\mathbf{r}))\delta v_{\text{loc}}(\mathbf{r})]d\mathbf{r}, \\ E^{\text{ion},\downarrow} &= \int [v_{\text{loc}}^o(\mathbf{r})n^{\downarrow}(\mathbf{r}) - \beta(\mathbf{r})(2 + \beta(\mathbf{r}))\delta v_{\text{loc}}(\mathbf{r})]d\mathbf{r}. \end{aligned} \quad (25)$$

The present theory has several advantages. First and foremost, it is very easy to add such a feature in any existing pseudopotential program that uses ultrasoft pseudopotentials. The method only requires adding a few lines of code and does not require the computation of any CPU-intensive extra terms, leading to a negligible overhead cost. Second, even though the spin-dependent formalism must be implemented in a real-space framework, we can conveniently evaluate the nonlocal contribution to the electron-ion energy in both reciprocal and real space as we like since the nonlocal projection operations are left unchanged. In particular, the latter operation in real space was shown to be computationally advantageous for large systems.²¹ Finally, we find that the method does not require more iterations of the self-consistent loop nor does it require a higher kinetic-energy cutoff for the plane-wave basis than for conventional pseudopotentials. A drawback, however, is that our new theory can only be considered at best as an approximation to a full implementation of the spin dependence where both local and nonlocal potentials would be perturbed. The results presented in the subsequent sections will show that, in fact, the discrepancies between both approaches are negligible.

IV. CALCULATIONAL DETAILS

We implemented our new method in the DFT plane-wave pseudopotential code CASTEP.^{22,23} We generated ultrasoft pseudopotentials for Cr, Ni, Fe, Co, and Pd with the parameters listed in Table I. The generation of such ultrasoft potentials is not an easy task, mainly because of the many parameter values to be chosen during the process. Therefore,

our approach has been to limit ourselves to the simplest and most systematic rationale: all cutoff parameters r_c for all channels have been set to the same value, and when a NLCC was employed, its cutoff value was automatically set equal to $0.7r_c$. We also have used the pseudopotentials provided by default with the CASTEP code. The corresponding generation parameters also are reported in Table I. All pseudopotentials were unscreened with the same exchange-correlation potential [LDA (Ref. 24) or GGA-PBE (Ref. 25)] as the one used for the crystal calculations. Their generation was performed by solving the Koelling-Harmon equation,²⁶ which includes scalar semirelativistic corrections (except for Cr and Ni), while a modified Troullier-Martins²⁷ scheme was used to create the ultrasoft pseudo-wave-functions.

All calculations were converged with respect to kinetic-energy cutoff and k -point sampling. For the bulk calculations, a k -point density of 0.04 \AA^{-3} was used throughout. The atomic calculations were performed by simulating an isolated atom, by placing the atom at the center of a large supercell ensuring no interactions with its periodic images, with no k -point sampling. Calculations also were performed for a Pd atomic wire, simulated by placing a Pd atom at the origin of a supercell of dimension $10 \text{ \AA} \times 10 \text{ \AA} \times a_o$, where a_o (in angstroms) is the interatomic distance in the linear chain of Pd atoms. For those calculations, we used a well-converged k -point mesh of $1 \times 1 \times 10$. All calculations were also converged with respect to plane-wave basis expansion, where the computational advantages of using USPPs for those transition metals are obvious since they allow one to use a basis set (and kinetic-energy cutoff) typically two or three times smaller than when using norm-conserving pseudopotentials. Our USPP never required a kinetic-energy cutoff larger than 400 eV to converge the total energy up to 0.05 eV/atom.

V. RESULTS

In order to benchmark our new spin-dependent ultrasoft pseudopotential theory, we present results for atomic Cr and Ni and some simple bulk metallic phases (fcc Ni, bcc Fe, and fcc Co), as well as a study of the magnetism in fcc Fe and in a linear chain of Pd atoms. Although we do report experimental data where available, our results really should be compared only with values given by all-electron theories since the pseudopotential approach is an approximation to the all-electron case. The fact that DFT, with its many approximations and parametrizations (mainly via the exchange-correlation potential chosen, either LDA or a flavor of the GGA), succeeds or fails to predict experimental values is another issue separate from whether PsP methods well approximate AE ones. The latter is the issue under consideration here.

A. Atomic benchmarks

As we mentioned earlier, the spin-dependent pseudopotentials were originally successfully implemented with norm-conserving pseudopotentials.^{15,17} In order to compare the results given by the rather different approach presented here, we first performed a couple of tests on isolated transition-

TABLE II. LSDA atomic-orbital energies for fully polarized Cr atom (in eV).

Orbital	Method				
	AE	SNP-I (US)	SDP-I (US)	SNP-II ^a (NC)	SDP-II ^a (NC)
$4s^\uparrow$	-4.56	-4.42	-4.53	-4.42	-4.54
$3d^\uparrow$	-3.98	-4.23	-3.97	-4.22	-3.97

^aReference 38.

metal atoms. Table II shows the orbital energies for the fully polarized Cr atom, as given by an AE calculation, by an ultrasoft spin-neutral pseudopotential (SNP-I), and by the corresponding spin-dependent pseudopotential (SDP-I). For the latter, we emphasize again that only the local potential is self-consistently updated. For comparison of the accuracy of our new method, we also display results given by a norm-conserving spin-neutral potential (SNP-II) and the spin-dependent pseudopotential (SDP-II), where both local and nonlocal potentials were self-consistently perturbed. Neither a NLCC nor semirelativistic corrections were included in these calculations. Table II demonstrates the failure of the conventional spin-neutral potentials to accurately predict orbital energies for highly polarized atomic Cr (s^1d^5), consistent with trends published previously for all first- and second-row transition elements.¹⁶ Note that even though the method used is different, both norm-conserving and ultrasoft pseudopotentials give consistent results, as expected. When the spin dependence is used, we see a fairly dramatic improvement of the results, with nearly perfect agreement with AE orbital energies. Most importantly, we can see that there is almost no discrepancy between the results given by a full spin-dependent pseudopotential (SDP-II) and our approximation of the method in the ultrasoft formalism (SDP-I), suggesting that our approximation to only perturb the local potential is indeed sufficient.

Table III displays results for Ni atom in its $4s^{1\uparrow,1\downarrow}3d^{5\uparrow,3\downarrow}$ and $4s^{1\uparrow,0\downarrow}3d^{5\uparrow,4\downarrow}$ electronic configurations. The orbital energies reported are those given by an AE method, an ultrasoft spin-neutral potential (SNP-I), and the associated spin-dependent one (SDP-I). For comparison purposes, we also included the results given by a full spin-dependent norm-conserving potential (SDP-II). Again, no NLCC or semirelativistic corrections have been included in those calculations. The results essentially show the same trend as the one discussed for atomic Cr, where the SNP-I fails at accurately reproducing AE orbital energies (except for the s orbitals), a failure that is nicely corrected by the inclusion of the spin dependence. Again, both ultrasoft and norm-conserving methods give essentially the same results, as expected within the calculational accuracy, and both are in consistently good agreement with the AE energies. In light of those results, we can conclude that for equivalent levels of theory, both norm-conserving and ultrasoft potentials give similar results, and that even though both spin-dependent formalisms (either fully perturbed norm-conserving or ultrasoft) are rather different, the physics captured by the theories remains the same.

TABLE III. LSDA atomic-orbital energies for Ni in the $4s^{1\uparrow,1\downarrow}3d^{5\uparrow,3\downarrow}$ and $4s^{1\uparrow,0\downarrow}3d^{5\uparrow,4\downarrow}$ electronic configurations (in eV). Acronyms are defined in the text (Sec. V A).

Configuration	Orbital	AE	Method		
			SNP-I (US)	SDP-I (US)	SDP-II ^a (NC)
$4s^{1\uparrow,1\downarrow}3d^{5\uparrow,3\downarrow}$	$4s^\uparrow$	-5.89	-5.86	-5.85	-5.86
	$4s^\downarrow$	-5.58	-5.51	-5.51	-5.55
	$3d^\uparrow$	-10.31	-11.01	-10.35	-10.24
	$3d^\downarrow$	-8.47	-7.63	-8.44	-8.39
$4s^{1\uparrow,0\downarrow}3d^{5\uparrow,4\downarrow}$	$4s^\uparrow$	-4.91	-4.98	-5.00	-4.96
	$4s^\downarrow$	-4.03	-4.10	-4.07	-4.07
	$3d^\uparrow$	-5.45	-5.85	-5.29	-5.37
	$3d^\downarrow$	-4.46	-4.14	-4.35	-4.37

^aReference 17.

B. Bulk Ni

We also performed calculations on bulk Ni in its face-centered-cubic (fcc) phase, using the same potentials as in the previous section for both the norm-conserving case (SNP-II and SDP-II) and the ultrasoft one (SNP-I and SDP-I). This case study was previously performed by Starrost *et al.*¹⁷ using the norm-conserving pseudopotentials SNP-II and SDP-II. Table IV reports the results for the bulk properties (equilibrium lattice constant a_o , bulk modulus B_o , and magnetic moment per atom in the cell μ_B) using the local spin-density approximation (LSDA), as parametrized by Perdew and Zunger.²⁸ For both SNP-I and SNP-II, the calculated bulk properties again yield similar results with an overestimated equilibrium lattice parameter and magnetic moment per atom. Only SNP-I seems to, perhaps fortuitously, give good agreement with the full-potential linearized augmented plane-wave (FLAPW) bulk modulus. Again, errors are reduced when the spin dependence is introduced, with a smaller predicted lattice parameter and a magnetic moment per atom in good agreement with the all-electron one. The bulk modulus, which may be a property intrinsically less sensitive to the spin polarization, does not show improvement in this case. These results, again meant for benchmarking of our new method against previous ones, show similar trends and results for the spin-dependent theory in both norm-conserving and ultrasoft formalisms.

TABLE IV. LSDA bulk properties of fcc Ni: lattice constant a_o , bulk modulus B_o , and magnetic moment per atom M . Acronyms are defined in Sec. V B of the text.

Method	a_o (Å)	B_o (GPa)	M (μ_B)
Experiment	3.52	184	0.62
AE FLAPW ^a	3.42	254	0.62
SNP-I (US)	3.46	254	0.80
SDP-I (US)	3.44	264	0.58
SNP-II (NC) ^b	3.49	209	0.77
SDP-II (NC) ^b	3.48	208	0.57

^aReference 30.^bReference 15.

C. Bulk Fe

We also applied our new method to the ground-state bcc phase of bulk Fe for both LSDA and spin-polarized GGA, although it is well known that failures of the LSDA incorrectly yield fcc Fe as the ground state.²⁹ Table V reports results for the LSDA and GGA equilibrium lattice parameters, bulk moduli, and magnetic moments per atom as given by various methods: all-electron FLAPW, our ultrasoft spin-neutral and spin-dependent pseudopotentials with and without NLCC (respectively, SNP-I and SDP-I or SNP-II and SDP-II), and pseudopotentials provided with the DFT code CASTEP (SNP-III, available for both LDA and GGA-PBE) as well as a previously reported result also using an ultrasoft potential (SNP-V). All our generated potentials include semi-relativistic corrections and all GGA results employ the PBE parametrization unless otherwise mentioned (the comparison between PW91 and PBE results is still a fair one since the former can be viewed as a superset of the latter, with both giving essentially the same results). Note also that SNP-III employs shorter cutoff radii than our pseudopotentials and is therefore expected to be of higher quality, but higher computational cost.

The overall failure of the conventional spin-neutral pseudopotentials is even more dramatic for bcc Fe than for fcc Ni. In both the LSDA and GGA cases, SNP-I gives very poor structural and magnetic properties. The inclusion of a NLCC in SNP-II improves the transferability of the potential and gives more reasonable results. Nevertheless, the introduction of the spin dependence is clearly the most effective strategy, whether or not a NLCC is included. Both SDP-I and SDP-II give essentially the same properties, in very good agreement overall with the predicted FLAPW values. The influence of the spin dependence has the most impact on magnetic properties, reducing the error produced by the spin-neutral potential within the LSDA from more than +60% (+30% if a NLCC is used) to less than +1% (-4% if a NLCC used). For GGA-PBE, the error drops from +56% (+23% if a NLCC is employed) to +4% (less than +2% with a NLCC). As for the other spin-neutral pseudopotentials, although

TABLE V. Ultrasoft pseudopotential and all-electron (FLAPW) LSDA and spin-polarized GGA bulk properties of bcc Fe: lattice constant a_o , bulk modulus B_o , and magnetic moment per atom M . Acronyms are defined in Sec. V C of the text.

XC type	Method	NLCC	a_o (Å)	B_o (GPa)	M (μ_B)
LSDA	Experiment		2.87	167	2.20
	FLAPW ^a	n/a	2.75	250	1.98
	SNP-I	No	2.95	151	3.24
	SDP-I	No	2.76	275	2.00
	SNP-II	Yes	2.83	198	2.59
	SDP-II	Yes	2.78	265	1.90
	SNP-III ^b	Yes	2.73	294	2.03
GGA	FLAPW ^c	n/a	2.84	174	2.17
	SNP-I	No	3.06	116	3.40
	SDP-I	No	2.86	198	2.26
	SNP-II	Yes	2.92	168	2.68
	SDP-II	Yes	2.86	198	2.20
	SNP-III ^b	Yes	2.81	219	2.21
	SNP-V ^d	Yes	2.86	157	2.32

^aReference 30.

^bDefault potential provided with the CASTEP program.

^cReference 30, using GGA-PW91.

^dReference 34, using GGA-PW91.

SNP-III gives very good results for the LSDA bcc phase, the GGA results are less impressive than when the spin dependence is employed. SNP-III yields properties that are less good at reproducing the AE values than the SDPs. These results lead us to conclude that the enhancement of the transferability due to the use of the spin-dependent pseudopotentials produces good bulk properties with or without a NLCC, and even with fairly large choices of the cutoff radii. Thus our theory allows for more accurate calculations at lower computational cost, with a minimum number of adjustable parameters.

The rich complexity of the competing magnetic phases of bulk Fe was pointed out previously by Herper *et al.*³⁰ and again by Jiang and Carter (JC).³¹ For example, AE DFT calculations within the FLAPW (Ref. 30) and PAW (Ref. 31) formalisms both predict that the ferromagnetic (FM) phase of fcc Fe exhibits a magnetic phase transition upon increasing volume from a low-spin FM phase to a high-spin FM phase. JC noted³¹ that the use of a high-quality, spin-neutral ultrasoft pseudopotential [from the VIENNA *ab initio* simulation package (VASP), denoted SNP-V herein] could not produce the correct phase ordering between those two FM phases of fcc Fe. In particular, AE methods such as PAW (Fig. 1, middle) predict the low-spin, small-volume phase to be lower in energy than the high-spin, large-volume phase, while SNP-V predicts precisely the reverse (Fig. 1, top). Moreover, the AE methods predict two antiferromagnetic (AF) phases, denoted as AF1 and AFMD, respectively, for single layer and double layer orderings of spins by Herper *et al.*,³⁰ to be lower in energy than either FM state, as illustrated by the PAW results of JC in Fig. 1(b). JC also attempted to use SNP-V to calculate the relative energy of one of the AF phases (AF1; see Fig. 1, top). Again, JC found that SNP-V produced qualitatively incorrect results in which the AF1 phase is predicted to be less stable than the high-spin FM phase. They did not bother calculating the AFMD phase,

expecting similar poor behavior of the pseudopotential.

In light of the qualitative discrepancies between predictions for FM and AF fcc Fe produced by the spin-neutral pseudopotential and those from all-electron calculations, this may be viewed as yet another important test case of the spin-dependent pseudopotential formalism. Figure 1 (bottom) displays the FM and AF states of fcc Fe (both AF1 and AFMD), as predicted by SDP-II. The results are strikingly similar to those from the AE calculations shown in Fig. 1(b), where the low-spin, small volume FM phase is favored over

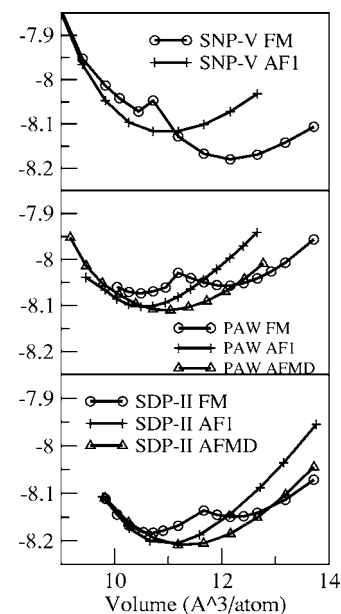


FIG. 1. DFT-GGA equations of state [cohesive energy (eV/atom) vs volume ($\text{\AA}^3/\text{atom}$)] for ferromagnetic (FM) and antiferromagnetic (AF1 and AFMD) phases of fcc Fe, calculated with (top) a spin-neutral ultrasoft pseudopotential (SNP-V from VASP; Jiang and Carter, unpublished results); (middle) the all-electron PAW method (Jiang and Carter within VASP; and (bottom) the ultrasoft spin-dependent pseudopotential method (SDP-II, this work).

TABLE VI. Pseudopotential and all-electron (LMTO) LSDA and GGA bulk properties of fcc Co: lattice constant a_o , bulk modulus B_o , and magnetic moment per atom M . All results are from ultrasoft pseudopotentials except as explicitly noted. Acronyms are defined in Sec. V D.

XC type	Method	NLCC	a_o (Å)	B_o (GPa)	M (μ_B)
LDA	Experiment		3.54	187	1.75
	AE LMTO ^a	n/a	3.46	255	1.62
	SNP-I	No	3.49	242	2.06
	SDP-I	No	3.43	255	1.53
	SNP-II	Yes	3.47	262	1.70
	SDP-II	Yes	3.45	255	1.48
	SNP-III ^b	No	3.54	234	2.05
	SNP-V ^c	Yes	3.45	242	1.52
	SDP-VI ^d	No	3.47	221	1.58
LAPW PsP ^e	FC	3.44	237	1.49	
GGA	AE LMTO ^a	n/a	3.54	244	1.68
	SNP-I	No	3.62	193	2.14
	SDP-I	No	3.54	206	1.61
	SNP-II	Yes	3.55	229	1.79
	SDP-II	Yes	3.54	221	1.64
	SNP-IV ^b	Yes	3.55	215	1.68

^aReference 33.

^bDefault potential provided with the CASTEP program.

^cReference 34.

^dNorm-conserving pseudopotential. Reference 17.

^eNorm-conserving pseudopotential with full core (FC). Reference 29.

the high-spin, large volume phase and the AF1 and AFMD phases are found to be lower in energy than the FM phase. Thus, the spin-dependent pseudopotential theory yields results of the same quality as the AE PAW formalism.

D. Bulk Co

We have performed LSDA and spin-polarized GGA calculations on the fcc phase of Co. Although Co has a hexagonal-close-packed (hcp) ground-state structure, its fcc and hcp properties are closely related and differences in cohesive energies between these two phases are very small.³² Furthermore, our main purpose is the comparison of pseudopotential methods with AE results, so the fact that we chose to study the fcc phase over its true experimental ground state is not important here. The results are shown in Table VI.

Within the LSDA, both SNP-I and SDP-I give fairly good structural properties when compared with all-electron linear muffin-tin orbital (LMTO) results,³³ but the spin-neutral potential once again tends to overestimate the magnetism. On the other hand, the use of spin dependence gives much better agreement with AE predictions and with results published by Starrost *et al.* (SDP-VI) (Ref. 17) using their full implementation of the spin-dependent pseudopotentials. When a NLCC is used, properties are improved for the spin-neutral potential as usual. In particular, the SNP-II yields a magnetic moment per Co atom of $1.70\mu_B$ compared to $1.62\mu_B$ predicted by the AE-LMTO method. By contrast, the SDP-II predicts a too low magnetic moment ($1.48\mu_B$), but a better bulk modulus. We also show for comparison the predictions of Moroni *et al.* using a high-quality pseudopotential,³⁴ as well as those from a LAPW pseudopotential method where the full core (FC) was used,²⁹ with the latter expected to give better results. Both methods also pre-

dict a low magnetic moment for the fcc phase of Co; the fact that our SDP-II yields results very close to the LAPW PsP ones suggests that the results given by our SDP-II are likely more trustworthy than the ones given by SDP-I. Finally, the default CASTEP potential SNP-III gives fairly poor structural and magnetic properties when compared to AE ones.

When the GGA-PBE is used, the predictions given by all methods are noticeably improved when compared to experiment. Although the potential SNP-I once again gives poor structural and magnetic properties compared to AE ones, the use of spin dependence gives good results, aside from a too low bulk modulus. When a NLCC is used in SNP-II, SDP-II, and SNP-IV, the results are generally good. Again, the use of the spin-dependent potential slightly improves upon the spin-neutral potential's transferability.

E. Pd atomic wire

The study of the properties of nanosystems is an emerging field of both basic and applied research with potentially interesting technological ramifications. In our last application of our new theory, we predict the properties of an infinitely long linear chain of Pd atoms, which recently has been proposed to exhibit magnetism.³⁵ Pd atomic wire magnetism is interesting because Pd is not an open-shell transition element in the isolated atom (its ground-state electronic configuration is d^{10}) and the ground-state crystal phase is nonmagnetic fcc. A possible explanation of potential magnetism in Pd atomic wires could be $d \rightarrow s$ transfer by symmetry breaking and probable $s-d$ hybridization to allow chemical bonding between Pd atoms. Very recently,^{35,36} two different DFT studies obtained conflicting results on whether a long Pd atomic wire exhibits magnetic ordering or not. While a DFT-GGA all-electron FLAPW calculation showed the wire could have

TABLE VII. Properties of a Pd wire (linear chain of atoms) as predicted by several DFT-GGA theories: interatomic distance a_o and magnetic moment per atom M (Bohr magneton).

Theory	NLCC	a_o (Å)	M (μ_B)
FLAPW	n/a	2.56	0.66
SNP-I	No	2.54	0.79
SDP-I	No	2.54	0.68
SNP-II	Yes	2.55	0.73
SDP-II	Yes	2.55	0.66
SNP-III ^a	No	2.48	0.80

^aDefault potential provided with the CASTEP program.

magnetic moments per atom up to $0.7\mu_B$, a prior DFT-GGA pseudopotential calculation failed to find the presence of any magnetism at all. We agree with the authors of the FLAPW study that those discrepancies could very well be due to the failure of the pseudopotential approximation for this specific case. As a result, we challenged our improved pseudopotential theory with this problem.

Here we have assumed an infinitely long linear chain of Pd atoms, where all atoms are uniformly spaced. With our three-dimensional periodic boundary conditions, we have simulated the atomic wire by placing a Pd atom at the origin of a supercell of dimensions $10 \text{ \AA} \times 10 \text{ \AA} \times a_o$, where a_o is the distance between two Pd atoms in the wire. We report in Table VII the distance a_o at which the total energy per Pd atom reaches a minimum, as well as its corresponding magnetic moment, as predicted by GGA-PBE. The details about the potentials used are also reported in Table I.

Surprisingly, we were unable to reproduce previously published findings using pseudopotential methods: all our potentials show non-negligible magnetic ordering of the Pd atomic wire. The potential SNP-III, however, seems to suffer from transferability issues, yielding a too short interatomic distance and an overestimated magnetic moment. For our ultrasoft pseudopotentials, the trend seen is very similar to the results discussed previously for other metals. While SNP-I produces a good interatomic distance, the magnetic moment per Pd atom is quite overestimated. As usual, including a NLCC tends to correct this to give better agreement with the FLAPW results. Nevertheless, in both cases where the spin-dependent pseudopotentials were employed, the results are greatly improved, leading to almost perfect agreement with AE values.

In Fig. 2 we show the variations of the magnetic moment of the Pd atomic wire as a function of interatomic distance. The FLAPW calculations predicted that such a profile should take the shape of a bell curve (see Fig. 2 in Ref. 35), with a magnetic moment as high as $0.7\mu_B$ and vanishing for interatomic distances shorter than 2.3 \AA or larger than 3.4 \AA . The rather poor results produced by SNP-III are evident here as well, where SNP-III gives magnetic properties in large disagreement with AE expectations. And although the results reported in Table VII for the SNP-I appeared better than SNP-III, we see that SNP-I also yields a poor profile, where the magnetic moment abruptly jumps to $0.8\mu_B$ and then stays roughly constant as the interatomic distance increases. Only the use of a NLCC and/or of the spin-dependent potentials

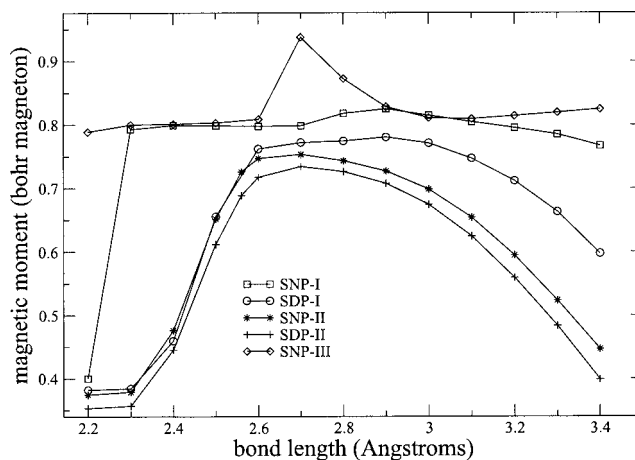


FIG. 2. GGA-PBE magnetic moment per atom as a function of interatomic distance for an infinitely long Pd atomic wire, as predicted by several pseudopotential methods.

corrects those inaccuracies, leading to curves resembling the AE one, with the best agreement found for the spin dependence used in conjunction with a NLCC. Unfortunately, all our potentials failed at reproducing the total quenching of the magnetic moment at the boundaries, further illustrating the extreme difficulty of this application for the pseudopotential approximation.

VI. CONCLUSIONS

The generation of pseudopotentials from first principles is in many ways a difficult task, in that the transferability and overall quality of the potential is extremely sensitive to the choice of its generation parameters. Many years of development have led to robust and efficient algorithms for generating optimally transferable pseudopotentials with very simple rules by which the values of such parameters can be conveniently chosen. Nevertheless, the unique properties of transition elements present additional challenges to the pseudopotential approximation, and the generation of such potentials often becomes somewhat of a “black art,” where the generally accepted practice is to tailor the value of the parameters until satisfactory benchmark results are met. We believe that this cannot be a satisfactory rationale for a first-principles method. Our goal is to systematically, without introduction of extra parameters, work toward an accurate, reliable, and more “*ab-initio*-like” pseudopotential theory. With such a spirit in mind, utilizing a perturbationlike approach employing multiple electronic reference states, the spin-dependent pseudopotentials were shown to markedly improve pseudopotential transferability for transition elements without introducing new parameters. In this paper, we have merged the spin-dependent pseudopotential theory with the computationally advantageous Vanderbilt ultrasoft pseudopotential method. We showed that it is easy to implement the spin dependence in any existing DFT code employing such potentials. Properties of both atomic and bulk systems for a variety of relevant transition metals show sensible improvement of the results when the perturbation is used, including when a nonlinear core correction has been applied. Because of the spin-dependent pseudopotential method, we were able to

generate potentials that produce good results when compared to all-electron ones, using fairly simple sets of nontweaked parameters, sets that would normally yield mild or poor accuracy. The success of this theory can be traced to the fact that the spin-dependent perturbation gives formally the correct limits for the majority of the valence electrons in both magnetic extremes: nonmagnetic and fully polarized atoms. Moreover, in some cases, and in agreement with previous findings,³⁷ the spin-dependent pseudopotentials give equal or better properties than potentials using shorter cutoff values, thereby providing us with an accurate, more *ab-initio*-like, and yet less expensive scheme that should prove useful for studying more complex magnetic materials in the future.

ACKNOWLEDGMENTS

The authors would like to thank the California NanoSystems Institute (CNSI) for computational time. We would also like to thank Professor Inder Batra for pointing out to us the problem of Pd atomic wires, as well as Dr. De-en Jiang for providing us with pseudopotential and PAW results for the ferromagnetic phases of bulk Fe. We are grateful to Accelrys for providing the CASTEP software. This work has been funded in part by the National Science Foundation, the Air Force Office of Scientific Research, and the Department of Energy, Basic Energy Sciences.

¹F. Abraham, J. Broughton, N. Berstein, and E. Kaxiras, *Comput. Phys.* **12**, 538 (1998).

²K. J. Caspersen, A. Lew, M. Ortiz, and E. A. Carter, *Phys. Rev. Lett.* **93**, 115501 (2004).

³M. Fago, R. L. Hayes, E. A. Carter, and M. Ortiz, *Phys. Rev. B* **70**, 100102 (2004).

⁴P. Hohenberg and W. Kohn, *Phys. Rev.* **136**, B864 (1964).

⁵W. Kohn and L. J. Sham, *Phys. Rev.* **140**, 1133 (1965).

⁶J. Ihm, A. Zunger, and M. L. Cohen, *J. Phys. C* **12**, 4409 (1979).

⁷W. E. Pickett, *Comput. Phys. Rep.* **9**, 115 (1989).

⁸P. E. Blöchl, *Phys. Rev. B* **50**, 17953 (1994).

⁹D. R. Hamann, M. Schlüter, and C. Chiang, *Phys. Rev. Lett.* **43**, 1494

(1979).

¹⁰D. Vanderbilt, *Phys. Rev. B* **41**, 7892 (1990).

¹¹I. Grinberg, N. J. Ramer, and A. M. Rappe, *Phys. Rev. B* **63**, 201102R (2001).

¹²D. Porezag, M. R. Pederson, and A. Y. Liu, *Phys. Rev. B* **60**, 14132 (1999).

¹³G. Kresse, W. Bergermayer, and R. Podloucky, *Phys. Rev. B* **66**, 146401 (2002).

¹⁴S. G. Louie, S. Froyen, and M. L. Cohen, *Phys. Rev. B* **26**, 1738 (1982).

¹⁵V. Cocula, F. Starrost, S. C. Watson, and E. A. Carter, *J. Chem. Phys.* **119**, 7659 (2003).

¹⁶S. C. Watson and E. A. Carter, *Phys. Rev. B* **58**, R13309 (1998).

¹⁷F. Starrost, H. Kim, S. C. Watson, E. Kaxiras, and E. A. Carter, *Phys. Rev. B* **64**, 235105 (2001).

¹⁸L. Kleinman and D. M. Bylander, *Phys. Rev. Lett.* **48**, 1425 (1982).

¹⁹K. Laasonen, A. Pasquarello, R. Car, C. Lee, and D. Vanderbilt, *Phys. Rev. B* **47**, 10142 (1993).

²⁰Note that our use of the superscript *o* differs from Vanderbilt's original notations. Our superscript always refers to spin-neutral quantities, whereas his refers to unscreened quantities. For example, by V^o , we mean the spin-neutral potential and not the unscreened potential.

²¹R. D. King-Smith, M. C. Payne, and J. S. Lin, *Phys. Rev. B* **44**, 13063 (1991).

²²M. C. Payne, M. P. Teter, D. C. Allan, T. A. Arias, and J. D. Joannopoulos, *Rev. Mod. Phys.* **64**, 1045 (1992).

²³M. D. Segall, P. J. D. Lindan, M. J. Probert, C. J. Pickard, P. J. Hasnip, S. J. Clark, and M. C. Payne, *J. Phys.: Condens. Matter* **14**, 2717 (2002).

²⁴D. M. Ceperley and B. J. Alder, *Phys. Rev. Lett.* **45**, 566 (1980).

²⁵J. P. Perdew, K. Burke, and M. Ernzerhof, *Phys. Rev. Lett.* **77**, 3865 (1996).

²⁶D. D. Koelling and B. N. Harmon, *J. Phys. C* **10**, 3107 (1977).

²⁷N. Troullier and J. L. Martins, *Phys. Rev. B* **43**, 1993 (1991).

²⁸J. P. Perdew and A. Zunger, *Phys. Rev. B* **23**, 5048 (1981).

²⁹J.-H. Cho and M. Scheffler, *Phys. Rev. B* **53**, 10685 (1996).

³⁰H. C. Herper, E. Hoffmann, and P. Entel, *Phys. Rev. B* **60**, 3839 (1999).

³¹D. E. Jiang and E. A. Carter, *Phys. Rev. B* **67**, 214103 (2003).

³²A. T. Paxton, M. Methfessel, and H. M. Polatoglou, *Phys. Rev. B* **41**, 8127 (1990).

³³M. Korling and J. Haglund, *Phys. Rev. B* **45**, 13293 (1992).

³⁴E. G. Moroni, G. Kresse, J. Hafner, and J. Furthmuller, *Phys. Rev. B* **56**, 15629 (1997).

³⁵A. Delin, E. Tossatti, and R. Weht, *Phys. Rev. Lett.* **92**, 057201 (2004).

³⁶S. R. Bahn and K. W. Jacobsen, *Phys. Rev. Lett.* **87**, 266101 (2001).

³⁷V. Cocula and E. A. Carter, *Phys. Rev. B* **69**, 052404 (2004).

³⁸V. Cocula, Master's thesis, University of California, Los Angeles, 2001.